

## Photoinitiated Destruction of Composite Porphyrin–Protein Polymersomes

Gregory P. Robbins,<sup>†</sup> Masaya Jimbo,<sup>‡,§</sup> Joe Swift,<sup>‡</sup> Michael J. Therien,<sup>§</sup> Daniel A. Hammer,<sup>⊥</sup> and Ivan J. Dmochowski<sup>‡,\*</sup>

*School of Engineering and Applied Sciences, Departments of Bioengineering and Chemical and Biomolecular Engineering, School of Arts and Sciences, University of Pennsylvania, Philadelphia, Pennsylvania 19104, Department of Chemistry, University of Pennsylvania, Philadelphia, Pennsylvania 19104, and Department of Chemistry, Duke University, Durham, North Carolina 27708*

Received November 2, 2008; E-mail: ivandmo@sas.upenn.edu

Polymersomes are bilayer vesicles assembled from block-copolymers, which can be varied to fine-tune polymersome strength and responsiveness.<sup>1–4</sup> Hydrophilic and hydrophobic solutes are readily incorporated within the aqueous interior or hydrophobic membrane, respectively. In the hydrophobic membrane, a variety of porphyrins have been incorporated at high concentrations<sup>5</sup> and used for *in vivo* fluorescence imaging.<sup>6,7</sup> Polymer vesicles that respond to external stimuli, serve as bioreactors, incorporate ATP synthase<sup>8</sup> and hemoglobin,<sup>9</sup> or recreate cellular organelle function have recently been reported.<sup>3,10–13</sup> Here, we describe the preparation and characterization of photoresponsive polymersomes which can release contents on optical cue; such materials would be useful for applications in biomedicine and engineering.

We describe the first example of a photoactive polymersome, which was formed by incorporating a protein in the aqueous interior and a meso-to-meso ethyne-bridged bis[porphyrinato]zinc (PZn<sub>2</sub>) chromophore in the membrane.<sup>14</sup> We initially investigated the encapsulation of horse spleen ferritin (HSF) or iron-free apoferritin (HSAF) inside a polyethylene oxide–polybutadiene (PEO<sub>30</sub>–PBD<sub>46</sub>, denoted OB29) diblock copolymer vesicle. Ferritins are large iron-storage proteins (MW ≈ 440 kDa) with 24 four-helix bundle subunits that form a 12-nm sphere with an 8-nm inner cavity. Ferritin sequesters up to 4500 iron atoms as a hydrous ferric oxide mineral core and can serve as a magnetic resonance imaging contrast agent.<sup>15–17</sup> We observed that ferritin incorporation drives the preferred polymersome morphology away from simple spheres toward asymmetric morphologies. Although some polymersomes remain spherical, increases in ferritin concentration lead to an increased frequency of polymersomes in nonspherical structures (Figure S1). The simultaneous incorporation of PZn<sub>2</sub> into the vesicle hydrophobic membrane imparts sensitivity to focused light of near-UV to near-IR wavelengths. Confocal laser scanning microscopy (CLSM) imaging of polymersomes loaded with both ferritin and PZn<sub>2</sub> at excitation wavelengths (488, 543, or 633 nm) where PZn<sub>2</sub> absorbs strongly<sup>14</sup> caused many of the vesicles to undergo irreversible morphological changes ranging from formation of new bends or “arms” and budding of smaller vesicles to total polymersome destruction (Figure 1). Similar results were seen during imaging by widefield fluorescence microscopy using a mercury arc lamp (Figure S2).

Formation of light-responsive polymersomes required the presence of protein and PZn<sub>2</sub> (Figures S3–S5). This phenomenon was observed in some polymersomes formed from solutions containing

as little as 1.5 mg/mL ferritin, but the fraction of vesicles that exhibited such photochemistry within a population, as well as the relative magnitude of the shape changes, generally increased with the ferritin concentration. Replacing HSF with HSAF, and conjugating a fluorophore (Cy3 or BODIPY-FL) to either protein, did not alter the photoresponse of the vesicles.

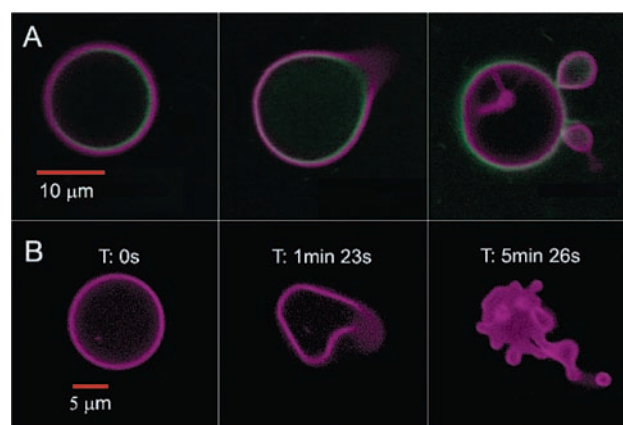


**Figure 1.** Confocal micrographs of polymersomes that membrane-disperse PZn<sub>2</sub> (purple) and encapsulate HSAF obtained in continuous scanning mode. (A) BODIPY-FL-labeled HSAF (green, 3 mg/mL) + PZn<sub>2</sub> vesicle, imaged using two lasers simultaneously (488, 543 nm). Images proceed in time, left to right, over a period of ~5 min. (B) Unlabeled HSAF (1.5 mg/mL) + PZn<sub>2</sub> vesicle. Vesicle imaged using three lasers simultaneously (488, 543, 633 nm). Final image of the degraded structure was not in the same plane as the original vesicle.

Ferritin was fluorescently labeled to study its interaction with the polymersome and understand how ferritin contributes to budding. CLSM imaging of samples containing Cy3- or BODIPY-FL-labeled ferritin confirmed the presence of protein within the polymersomes (Figures 2A and S6). Encapsulated BODIPY-FL-labeled ferritin localized to the membrane (Figure 1A), whereas Cy-3 labeled ferritin was found both at the membrane and dispersed throughout the aqueous core. BODIPY-FL is a neutral dye; therefore, we surmise that unlabeled ferritin also localizes at the membrane. In contrast, Cy3 has a net negative (–1) charge, which may contribute to ferritin partitioning between the aqueous core and hydrophobic membrane.

Experiments were performed to determine if ferritin is unique in affecting polymersome morphology. Bovine serum albumin (BSA) or equine skeletal myoglobin (Mb) were loaded at either 1.5 or 10 mg/mL by the same procedure used for ferritin. Other groups previously loaded BSA into the interior of polymer vesicles but did not observe changes to the shape of static vesicles in the absence of porphyrin.<sup>18</sup> Polymersomes incorporating PZn<sub>2</sub> and 1.5

<sup>†</sup> Dept. of Chemical and Biomolecular Engineering, University of Pennsylvania.

<sup>‡</sup> Dept. of Chemistry, University of Pennsylvania.

<sup>§</sup> Dept. of Chemistry, Duke University.

<sup>⊥</sup> Depts. of Chemical and Biomolecular Engineering and Bioengineering, University of Pennsylvania.

\* Currently at Jefferson Medical College, Philadelphia, PA.

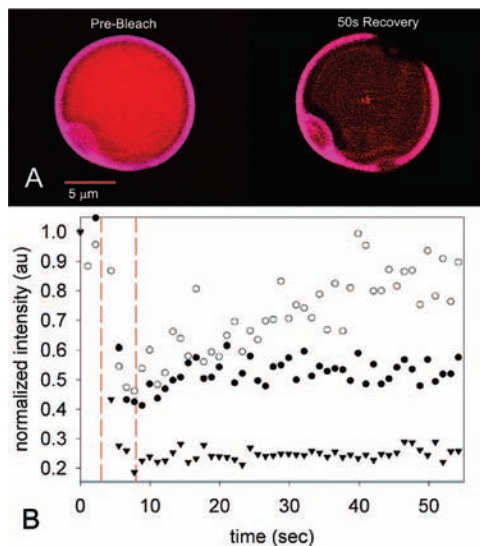


**Figure 2.** FRAP experiments on vesicles containing 1.5 mg/mL Cy3-labeled HSAF and PZn<sub>2</sub>. (A) No Cy3 or PZn<sub>2</sub> fluorescence recovery observed at the membrane, whereas (B) plot of Cy3 intensity in the aqueous core shows recovery after photobleaching. PZn<sub>2</sub> emission intensity at the membrane did not recover and is plotted as a reference. Photobleaching (351 nm, small region of interest) occurred during the time period indicated by dashed vertical lines. ● = Cy3-membrane, ○ = Cy3-aqueous core, ▼ = PZn<sub>2</sub>-membrane.

or 10 mg/mL BSA or Mb also experienced laser-induced shape changes, although the response was less dramatic than seen in the ferritin–PZn<sub>2</sub> system (Figure S7). The magnitude of photoinduced shape change was smallest in the BSA–PZn<sub>2</sub> vesicles, with only vesicle elongation observed. CLSM images of vesicles loaded with BODIPY-FL-labeled Mb or BSA showed that Mb associated predominantly with the polymer membrane, whereas BSA was also present throughout the aqueous core (data not shown).

We hypothesized that the internal protein could be modulating the morphological changes by adsorbing to the inner membrane, in which case the protein mobility should be greatly reduced. Fluorescence recovery after photobleaching (FRAP) experiments with vesicles containing only PZn<sub>2</sub> confirmed that the motion of these fluorophores within the membrane was restricted, with no PZn<sub>2</sub> fluorescence recovery observed 1 min after photobleaching (Figure 2). FRAP experiments performed on vesicles containing both fluorescently labeled ferritin and PZn<sub>2</sub> showed similarly restricted diffusion of PZn<sub>2</sub> at the membrane. In all FRAP studies, polymersomes containing HSF behaved similarly to vesicles containing HSAF (Figure S8). For polymersomes containing PZn<sub>2</sub> and the more dispersed Cy3-labeled HSAF, FRAP was measured at two locations: the vesicle membrane and the aqueous core. Significant recovery of Cy3 fluorescence was observed in the aqueous core (Figures 2B and S7D). However, no significant Cy3 fluorescence recovery was observed upon bleaching at the membrane (Figures 2A and S7E), indicating slow exchange between HSAF molecules in the membrane and these proteins in the aqueous core. Restricted diffusion at the membrane was also observed with BODIPY-labeled HSAF.

Flow cytometry (Figure S9) confirmed what had been observed during CLSM imaging of single ferritin–PZn<sub>2</sub> vesicles. The average amount of ferritin encapsulated in a population of vesicles scaled with increasing ferritin concentration in the hydration buffer as well as with vesicle size. These experiments also confirmed that the amount of ferritin encapsulated in a population of uniform-size vesicles can vary significantly.

Micropipette aspiration<sup>2,5</sup> was performed on composite vesicles to characterize the effect of ferritin encapsulation on polymersome membrane strength (Figure 3). All vesicles aspirated with pipettes 5 μm or smaller in diameter ruptured. When tensions were exerted on the membranes of similar vesicles using larger pipettes (>7 μm I.D.), vesicles could be aspirated intact. These data indicated that the bending rigidity of vesicle membranes was altered by the incorporation of ferritin. Both the average elastic modulus ( $K_a$ ) of a population and the range of moduli within a population increased with ferritin concentration. These results are consistent with protein association with the vesicle membrane.

Proteins and polypeptides have previously been encapsulated within polymersomes, but there has been relatively little characterization of the protein–membrane interactions in these systems.<sup>8,9,18,19</sup> In this example, the 9.6-nm OB29 bilayer hydrophobic core is too thin to incorporate holo-ferritin (12-nm O.D.). Complete intercalation into the membrane would be possible only if the stable 24-mer ferritin dissociated into subunits. Thus, we hypothesize that internalized ferritin can associate with but not fully intercalate into the polymer membrane.

Observations of budding from CLSM suggest that the shape changes are caused by localized heating due to sample absorption of focused light within the membrane. Adsorption of protein on the inner membrane appears to cause differential rigidification of the membrane leaflets; shape change and budding then releases the stress on the membrane that results from heat energy localized between the two leaflets. Support for local heating comes from the observation that no budding occurred when vesicles loaded with PZn<sub>2</sub> and ferritin were kept in the dark and heated to 45 °C on a

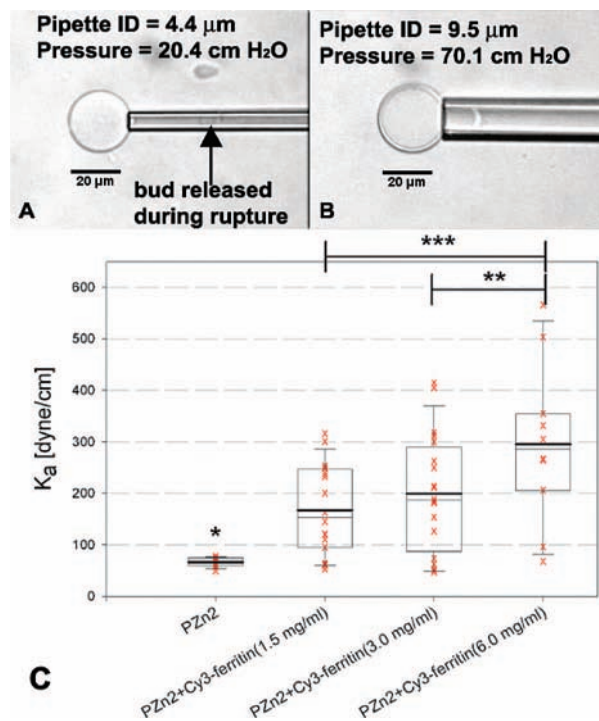


**Figure 3.** Micropipette aspiration on composite vesicles. (A) Experiments with small pipettes (ID < 5 μm) result in rupture at low tensions, while (B) vesicles remain intact at high tensions in experiments with larger pipettes. (C) Elastic modulus,  $K_a$ , of vesicles incorporating PZn<sub>2</sub> and Cy3-labeled ferritin at various hydration concentrations. The mean (bold line) and median (thin line) are indicated within the boxes. The box indicates the middle 50% of the range, while the whiskers indicate 95% and 5% of the range of measured  $K_a$  values. One-sided *t* test used to compare samples; \* = 99.999% confidence compared to each ferritin-incorporating sample, \*\* = 95% confidence, \*\*\* = 98% confidence.

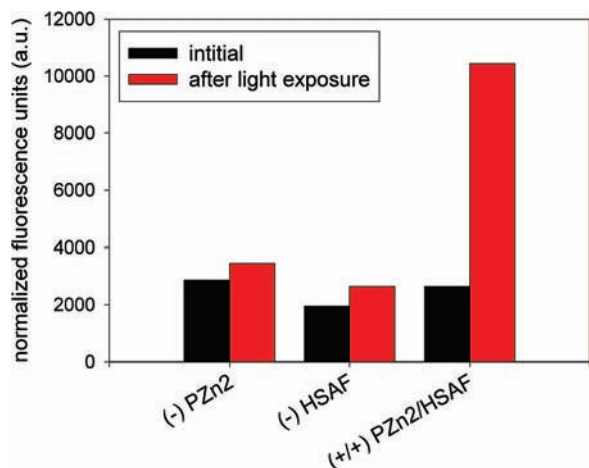


**Figure 4.** Fluorescence assay shows significant increase of solution biocytin for only HSAF + PZn<sub>2</sub> sample, which is released upon 4-h vesicle irradiation using a Hg arc lamp.

microscope stage. PZn<sub>2</sub> chromophores absorb across the near-UV and visible spectrum and possess an intense near-infrared absorbance feature.<sup>14</sup> With a fluorescence quantum yield of 16%, most of the absorbed energy is dissipated by PZn<sub>2</sub> as heat. The local “hotspot” mechanism was also proposed in recent work with gold nanoparticle-loaded vesicles.<sup>20,21</sup> PZn<sub>2</sub> photochemistry is not likely involved in this process, as excited PZn<sub>2</sub> species undergo little intersystem crossing and are poor photosensitizers for dioxygen.<sup>14</sup> Moreover, PZn<sub>2</sub>-only control vesicles are nonresponsive and substitution of PZn<sub>2</sub> with Nile Red produced fluorescent vesicles that were not photoresponsive (Figure S10). Thus, it is unlikely that vesicle shape changes were caused by <sup>1</sup>O<sub>2</sub>. Because the PZn<sub>2</sub> barrier to rotation around the ethynyl bridge is significant when embedded in the polymersome membrane,<sup>22</sup> we rule out excited-state conformational changes of PZn<sub>2</sub> as a factor contributing to the observed shape changes.

Finally, experiments were performed to demonstrate photorelease of a small-molecule “drug” (biocytin) from ferritin–PZn<sub>2</sub> vesicles (Figure 4). Solutions of vesicles were exposed to light from a Hg arc lamp for 4 h (~20 W at sample). Fluorescence quantitation of biocytin in solution was performed using a secondary protein, and results were normalized based on vesicle concentration as determined by PZn<sub>2</sub> absorbance prior to release. These initial experiments show that 25–50% of encapsulated biocytin is released from vesicles. Release can be increased by optimizing the composite vesicle system.

In conclusion, a tertiary system of polymersome–protein–PZn<sub>2</sub> chromophore was shown to undergo vesicle shape changes upon exposure to light. The data indicate synergy between protein, which is in the vesicle interior, and PZn<sub>2</sub>, which embeds in the membrane, harvests light energy and produces local heating that leads to membrane budding. This effect was most pronounced with ferritin

but was also observed with Mb and BSA. The broad range of wavelengths that induce vesicle deformation in these systems suggests local membrane heating mediated by electronically and vibrationally excited porphyrin molecules, whose photophysical properties can be tuned through synthetic modifications.<sup>14</sup> Given the established exceptional NIR absorptivity of PZn<sub>2</sub> and closely related chromophores,<sup>14</sup> it may be possible to harness light-activated vesicle destruction for in vivo, targeted drug delivery.

**Acknowledgment.** The authors acknowledge NSF MRSEC DMR-0520020 (to I.J.D., D.A.H., and M.J.T.) and NSF CAREER CHE-0548188 and NCRR 1S10-RR-021113-01 (to I.J.D.) for funding. We thank Samuel Bernard, Shraddha Ranka, and Natalie Christian for preliminary studies and Roderic Eckenhoff and Jasmina Cheung-Lau for HSAF. Eric Johnston provided valuable help with micropipette aspiration studies.

**Supporting Information Available:** Materials and methods, additional figures. Three AVI files showing polymersome deformation and destruction in time series of confocal micrographs. This material is available free of charge via the Internet at <http://pubs.acs.org>.

## References

- (1) Discher, B. M.; Won, Y. Y.; Ege, D. S.; Lee, J. C. M.; Bates, F. S.; Discher, D. E.; Hammer, D. A. *Science* **1999**, *284*, 1143–1146.
- (2) Bermudez, H.; Brannan, A. K.; Hammer, D. A.; Bates, F. S.; Discher, D. E. *Macromolecules* **2002**, *35*, 8203–8208.
- (3) Bhargava, P.; Tu, Y. F.; Zheng, J. X.; Xiong, H. M.; Quirk, R. P.; Cheng, S. Z. D. *J. Am. Chem. Soc.* **2007**, *129*, 1113–1121.
- (4) Ortiz, V.; Nielsen, S. O.; Klein, M. L.; Discher, D. E. *J. Polym. Sci. Polym. Phys.* **2006**, *44*, 1907–1918.
- (5) Ghoroghchian, P. P.; Lin, J. J.; Brannan, A. K.; Frail, P. R.; Bates, F. S.; Therien, M. J.; Hammer, D. A. *Soft Matter* **2006**, *2*, 973–980.
- (6) Ghoroghchian, P. P.; Frail, P. R.; Susumu, K.; Blessington, D.; Brannan, A. K.; Bates, F. S.; Chance, B.; Hammer, D. A.; Therien, M. J. *Proc. Natl. Acad. Sci. U.S.A.* **2005**, *102*, 2922–2927.
- (7) Christian, N. A.; Milone, M. C.; Ranka, S. S.; Li, G. Z.; Frail, P. R.; Davis, K. P.; Bates, F. S.; Therien, M. J.; Ghoroghchian, P. P.; June, C. H.; Hammer, D. A. *Bioconjugate Chem.* **2007**, *18*, 31–40.
- (8) Choi, H. J.; Montemagno, C. D. *Nano Lett.* **2005**, *5*, 2538–2542.
- (9) Arifin, D. R.; Palmer, A. F. *Biomacromolecules* **2005**, *6*, 2172–2181.
- (10) Geng, Y.; Discher, D. E. *J. Am. Chem. Soc.* **2005**, *127*, 12780–12781.
- (11) Qin, S. H.; Geng, Y.; Discher, D. E.; Yang, S. *Adv. Mater.* **2006**, *18*, 2905.
- (12) Ben-Haim, N.; Broz, P.; Marsch, S.; Meier, W.; Hunziker, P. *Nano Lett.* **2008**, *8*, 1368–1373.
- (13) Vriezema, D. M. L. P. M.; Garcia, N.; Oltra, S.; Hatzakis, N. S.; Kuiper, S. M. M.; Nolte, R. J.; Rowan, A. E.; van Hest, J. C. M. *Angew. Chem., Int. Ed.* **2007**, *46*, 7378–7382.
- (14) Duncan, T. V.; Susumu, K.; Sinks, L. E.; Therien, M. J. *J. Am. Chem. Soc.* **2006**, *128*, 9000–9001.
- (15) Harrison, P. M.; Arosio, P. *BBA-Bioenergetics* **1996**, *1275*, 161–203.
- (16) Theil, E. C. *J. Nutr.* **2003**, *133*, 1549S–1553S.
- (17) Bulte, J. W.; Douglas, T.; Mann, S.; Frankel, R. B.; Moskowitz, B. M.; Brooks, R. A.; Baumgarner, C. D.; Vymaza, I. J.; Strub, M. P.; Frank, J. A. *J. Magn. Reson. Imag.* **1994**, *4*, 497–505.
- (18) Wittemann, A.; Azzam, T.; Eisenberg, A. *Langmuir* **2007**, *23*, 2224–2230.
- (19) Shnyrova, A. V.; Ayllon, J.; Mikhalyov, I. I.; Villar, E.; Zimmerberg, J.; Frolov, V. A. *J. Cell Biol.* **2007**, *179*, 627–633.
- (20) Passonen, L.; Laaksonen, T.; Johans, C.; Yliperttula, M.; Kontturi, K.; Urtti, A. *J. Controlled Release* **2007**, *122*, 86.
- (21) Wu, G.; Mikhailovsky, A.; Khant, H. A.; Fu, C.; Chiu, W.; Zasadzinski, A. J. *Am. Chem. Soc.* **2008**, *130*, 8175.
- (22) Duncan, T. V.; Ghoroghchian, P. P.; Rubstov, I. V.; Hammer, D. A.; Therien, M. J. *J. Am. Chem. Soc.* **2008**, *130*, 9773–9784.

JA808586Q